

## MIT Open Access Articles

*Capacities of linear quantum optical systems*

The MIT Faculty has made this article openly available. **Please share** how this access benefits you. Your story matters.

**Citation:** Lupo, Cosmo et al. "Capacities of Linear Quantum Optical Systems." Physical Review A 85.6 (2012): 062314. © 2012 American Physical Society.

**As Published:** <http://dx.doi.org/10.1103/PhysRevA.85.062314>

**Publisher:** American Physical Society

**Persistent URL:** <http://hdl.handle.net/1721.1/73517>

**Version:** Final published version: final published article, as it appeared in a journal, conference proceedings, or other formally published context

**Terms of Use:** Article is made available in accordance with the publisher's policy and may be subject to US copyright law. Please refer to the publisher's site for terms of use.



# Capacities of linear quantum optical systems

Cosmo Lupo,<sup>1</sup> Vittorio Giovannetti,<sup>2</sup> Stefano Pirandola,<sup>3</sup> Stefano Mancini,<sup>1,4</sup> and Seth Lloyd<sup>5</sup>

<sup>1</sup>*School of Science and Technology, University of Camerino, I-62032 Camerino, Italy*

<sup>2</sup>*NEST, Scuola Normale Superiore and Istituto Nanoscienze-CNR, I-56126 Pisa, Italy*

<sup>3</sup>*Department of Computer Science, University of York, York YO10 5GH, United Kingdom*

<sup>4</sup>*INFN-Sezione di Perugia, I-06123 Perugia, Italy*

<sup>5</sup>*Department of Mechanical Engineering, MIT Cambridge, Massachusetts 02139, USA*

(Received 23 January 2012; published 19 June 2012)

A wide variety of communication channels employ the quantized electromagnetic field to convey information. Their communication capacity crucially depends on losses associated to spatial characteristics of the channel such as diffraction and antenna design. Here we focus on the communication via a finite pupil, showing that diffraction is formally described as a *memory channel*. By exploiting this equivalence we then compute the communication capacity of an optical refocusing system, modeled as a converging lens. Even though loss of information originates from the finite pupil of the lens, we show that the presence of the refocusing system can substantially enhance the communication capacity. We mainly concentrate on communication of classical information, the extension to quantum information being straightforward.

DOI: [10.1103/PhysRevA.85.062314](https://doi.org/10.1103/PhysRevA.85.062314)

PACS number(s): 03.67.Hk, 42.50.Ex, 42.30.—d

## I. INTRODUCTION

The most prominent candidate for implementing long-distance quantum communication is undoubtedly represented by the electromagnetic field (EMF) [1]. Although quantum information theory is more commonly represented in terms of discrete variables (e.g., qubits), information is most naturally encoded in the EMF by means of continuous variables, which, in the quantum domain, are described by bosonic degrees of freedom. Moreover, all the fundamental quantum information tools and protocols have been demonstrated for continuous variable systems [2,3], from quantum computation [4] to quantum error correction [5,6], quantum teleportation [7], and quantum key distribution [8–10]. Here we consider the problem of optical quantum communication [11–13], and compute the communication capacity, that is, the maximum rate at which information can be reliably transmitted. Although we explicitly consider communication of classical information [14], our results are immediately extensible to the case of quantum information [15].

The most general and simple, although physically relevant, mathematical model of optical communication line is the Gaussian channel [16], which describes the linear propagation of the EMF. In the classical domain, the ultimate limits for communication via Gaussian channels were provided by the seminal work of Shannon [17]. In the quantum domain, the structure of Gaussian channels is notably rich [18], with nontrivial properties in terms of degradability [19] and security [20,21]. However, a full information theoretical characterization has been presently achieved only for certain families of channels, such as the lossy channel [22–24]. These results have been applied to compute the maximum rate of reliable communication via attenuating media, as optical fibers, wave guides, and via free-space propagation [13,25,26]. Moving along this line we provide the information theoretical description of the effects of the signal propagation through lossy communication channels with linear characteristic. After introducing the general methods, we consider the example of an optical refocusing system with finite pupil, which is

schematized as a thin lens which is placed between the sender of the message and the receiver under focusing conditions. Notwithstanding its relatively simple structure this setup captures the basics features of all those situations in which a transmitted signal is either focused on a detector by a suitable optical system prior to the information decoding process, or where it has to be refocused by a suitable repeater to allow long-distance communication, for example, by means of parabolic antenna for satellite communication [27].

We explicitly discuss how the signal diffraction through the optical system can be formally described as a quantum channel with correlated noise (*memory channel*) [28], where correlations are quantified in terms of the associated Rayleigh length. Therefore, the information theoretical characterization of the resulting quantum channel is carried out using tools and methods that have been previously applied to quantum memory channels [29]. In this framework the main effect of the signal propagation through the optical system is to introduce the diffraction of light caused by its finite pupil, leading to bandwidth limited communication [30]. However, when compared with the free-space communication scheme [26], the presence of the refocusing apparatus may yield an improvement in the channel capacity of the system. This possibility has been put forward in Ref. [31]. Here we provide a detailed derivation of the channel model together with the analysis of results in several configurations. Furthermore, we also extend the approach to encompass the case of nonmonochromatic light.

The article proceeds as follows. In Sec. II, we provide the general model for communication via lossy multimode quantum optical channels. In Sec. III, we introduce a simplest example of such a system, communication through a converging lens with finite pupil, and show that it can be formally described as a channel with correlated noise. In Sec. IV we quantize this system, whose communication capacity is computed in Sec. V for the case of monochromatic light. We then compare the communication via the refocusing system with the free-space setting in Sec. VI. Section VII is devoted

to the extension to the nonmonochromatic case, and Sec. VIII is for final remarks.

## II. COMMUNICATION CAPACITY OF QUANTIZED LINEAR OPTICAL SYSTEMS

Consider a linear optical system with a set of  $M$  transmitter modes, labeled by  $i$ , and  $N$  receiver modes, labeled by  $j$ . In the case of radio-frequency or microwave communication, for example, the transmitter and receiver could be antennae. For optical communication, the transmitter could be a laser coupled to a telescope, and the receiver could be a telescope coupled to a charge-coupled-device (CCD) array. Transmitter and receiver modes typically have both spatial characteristics determined by the optical properties of the setup, and temporal characteristics, determined by the frequency and bandwidth of the radiation employed in the communication. The transmittivity matrix  $T_{ji}$  gives the fraction of light from the  $i$ th transmitter mode that is received at the  $j$ th receiver mode. We would like to determine the maximum amount of information that can be sent for fixed total input power.

First, consider the purely lossy case, in which noise from the environment is negligible. This is the case, for example, for free-space optical communication in a thermal background. The addition of noise is considered below. When there is just one transmitter mode and one receiver mode, the channel is simply the lossy bosonic channel, whose classical capacity is known [22]: If the loss is  $\eta$  and the single-use average photon number is  $\bar{n}$ , then the number of *bits* that can be sent down the channel is  $g(\eta\bar{n})$ , where

$$g(x) := \begin{cases} (x+1)\log_2(x+1) - x\log_2 x & \text{for } x > 0, \\ 0 & \text{for } x \leq 0. \end{cases} \quad (1)$$

The capacity is attained by sending coherent states down the channel. If there are  $M$  parallel channels, with average photon number  $\bar{n}_i$  for the  $i$ th channel, then the capacity is simply the sum of the capacities for the individual channels.

In our case, we have a single multimode lossy channel with transmittivity matrix  $T_{ji}$ , which mixes the input modes together. This channel can be transformed into a set of parallel channels by using the singular value decomposition. The singular value decomposition states that any  $N \times M$  matrix  $T$  can be written as

$$T = \mathcal{V}\Sigma\mathcal{U}, \quad (2)$$

where  $\mathcal{V}$  is an  $N \times N$  unitary matrix,  $\Sigma$  is an  $N \times M$  matrix with entries only on the diagonal, and  $\mathcal{U}$  is an  $M \times M$  unitary matrix. In our case, we can write the transmittivity matrix  $T$  in components as

$$T_{ji} = \sum_k \mathcal{V}_{jk} \sqrt{\eta_k} \mathcal{U}_{ki}, \quad (3)$$

where  $\{\sqrt{\eta_k}\}$  are the singular values of the transmittivity matrix. The singular value decomposition shows that any multimode lossy channel can be decomposed into parallel lossy channels with input modes corresponding to the rows of  $\mathcal{U}$ , output modes corresponding to the columns of  $\mathcal{V}$ , and loss factors corresponding to the singular values  $\eta_k$ .

The singular value input modes can now be quantized using annihilation and creation operators  $a_j, a_j^\dagger$ :  $[a_j, a_{j'}^\dagger] =$

$\delta_{j,j'}$ . Similarly, the output modes can be quantized using annihilation and creation operators  $b_j, b_j^\dagger$ :  $[b_j, b_{j'}^\dagger] = \delta_{j,j'}$ . To preserve the canonical quantization relationships, each input-output pair is coupled to an environment mode with annihilation and creation operators  $\xi_j, \xi_j^\dagger$ :

$$b_j = \sqrt{\eta_j} a_j + \sqrt{1-\eta_j} \xi_j. \quad (4)$$

We see that the singular value decomposition of the multimode lossy quantum channel renders the channel completely equivalent to a set of parallel lossy quantum channels with loss factors  $\eta_j$ . The communication capacity of the channel when  $\bar{n}_j$  photons are transmitted down the  $j$ th singular value mode is simply  $\sum_j g(\eta_j \bar{n}_j)$ .

If the  $j$ th singular value mode has average energy per photon  $\hbar\bar{\omega}_j$ , then the capacity of the channel with total energy  $E$  per use is obtained by solving the constrained maximization problem with Lagrangian

$$\sum_j g(\eta_j \bar{n}_j) - \mu \left( \sum_j \bar{n}_j \hbar\bar{\omega}_j - E \right), \quad (5)$$

yielding the solution

$$\bar{n}_j = [\eta_j (2^{\mu \hbar\bar{\omega}_j / \eta_j} - 1)]^{-1}. \quad (6)$$

Here, the Lagrange multiplier  $\mu$  is chosen to give the proper total energy  $E$ . In the following, when dealing with monochromatic light, we express the energy in terms of number of photons,  $\bar{n} = E/(\hbar\omega)$ .

Thus, the singular value decomposition allows us to transform any linear, lossy, multimode channel with transmittivity matrix  $T_{ji}$  into a set of parallel lossy channels. Quantization then yields the capacity of this set of parallel channels. We now apply this result to various simple optical settings. In particular, we show that the resulting capacity can be significantly larger than the capacity which is achieved by using “naive” coding and decoding techniques.

## III. THE OPTICAL SYSTEM

We consider the propagation of light along an optical axis  $z$ . The input and output signals are identified by the transverse light fields at two planes orthogonal to the optical axis, respectively identified as the object plane and image plane [see Fig. 1(a)]. In classical scalar optics, the monochromatic optical fields at the object and image plane are described by scalar functions  $U_o(\mathbf{r}_o)$ ,  $U_i(\mathbf{r}_i)$ , where  $\mathbf{r}_o$  and  $\mathbf{r}_i$  are the Cartesian coordinates at the object and image plane. For linear systems, including the free-space propagation of light, the input/output relations at the object and image planes, respectively, are described by a transfer function  $T(\mathbf{r}_i, \mathbf{r}_o)$ , such that

$$U_i(\mathbf{r}_i) = \iint d^2\mathbf{r}_o T(\mathbf{r}_i, \mathbf{r}_o) U_o(\mathbf{r}_o). \quad (7)$$

The quantum version of the relations (7) can be derived by applying the canonical quantization procedure and introducing a proper set of normal modes for the input and output fields (as is done in Ref. [13] for the free-space propagation).

As mentioned in the Introduction, we model the optical refocusing system as a converging lens of focal length  $f$ ,

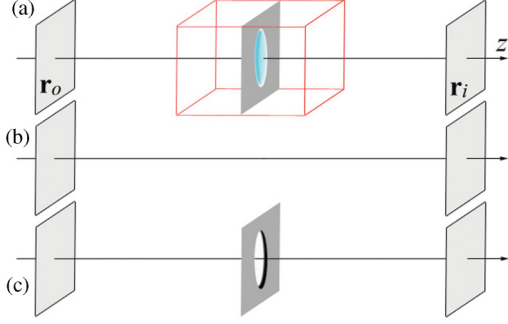


FIG. 1. (Color online) (a) Optical communication through an optical refocusing apparatus, modeled as a thin lens of radius  $R$  and focal length  $f$ . (b) The free-space propagation scenario. (c) An alternative scenario in which the lens is replaced by a hole of the same size in the absorbing screen.  $\mathbf{r}_o$  and  $\mathbf{r}_i$  denote the Cartesian coordinates on the object and image planes, respectively.

located at distance  $D_o$  from the object plane. Working in the thin lens, paraxial approximation, and neglecting aberrations, light is collected at the image plane located at distance  $D_i$  from the optical system, where  $1/D_o + 1/D_i = 1/f$ . Eventually the image is magnified by a factor  $M = D_i/D_o$ . Diffraction of light is responsible for image blurring and causes loss of information. It can be described by introducing an effective entrance pupil characterizing the optical system. Denoting  $P(\mathbf{r})$  the characteristic function of the pupil that encircles the lens, the transfer function for the monochromatic field of wavelength  $\lambda$  is obtained by Fourier transforming [32]:

$$T(\mathbf{r}_i, \mathbf{r}_o) = \frac{e^{i\vartheta(\mathbf{r}_i, \mathbf{r}_o)}}{\lambda^2 D_o D_i} \iint d^2\mathbf{r} P(\mathbf{r}) e^{-i2\pi \frac{(\mathbf{r}_i - M\mathbf{r}_o)}{\lambda D_i} \cdot \mathbf{r}} \quad (8)$$

(throughout the paper  $i$  denotes the imaginary unit). In writing the above expression we are implicitly assuming that the light rays which do not hit the pupil will not reach the image plane (either because they are scattered out, or because they are absorbed by some medium). Such hypothesis is not fundamental and could be dropped by adding an extra term to Eq. (8), which accounts for the diffraction of the light rays that miss the pupil. Eventually, we notice that, in the paraxial approximation, the acquired phase results

$$\vartheta(\mathbf{r}_i, \mathbf{r}_o) = \frac{\pi}{\lambda D_o} (|\mathbf{r}_o|^2 + |\mathbf{r}_i|^2/M) + \frac{2\pi D_o}{\lambda} (1 + M). \quad (9)$$

For instance, in the case of a circular lens of radius  $R$ , the pupil function is

$$P(\mathbf{r}) = \begin{cases} 1 & \text{for } |\mathbf{r}| < R, \\ 0 & \text{for } |\mathbf{r}| > R, \end{cases} \quad (10)$$

and the transfer function reads

$$T(\mathbf{r}_i, \mathbf{r}_o) = \frac{e^{i\vartheta(\mathbf{r}_i, \mathbf{r}_o)} R^2}{\lambda^2 D_o D_i} \frac{J_1(2\pi R\rho)}{R\rho}, \quad (11)$$

where  $J_1$  indicates the Bessel function of first kind and order one, and  $\rho := |\mathbf{r}_i - M\mathbf{r}_o|/(\lambda D_i)$ .

#### A. Light diffraction as a memory channel

We shall see that the effects of diffraction on light propagation can be described as memory effects in the communication

channel. Let us recall that a *memoryless* channel is such that its action on different channel inputs are identical and independent. Conversely, the actions of a *memory channel*, also called a *channel with correlated noise*, at different uses are not independent and/or not identical.

Let us assume that information is encoded at the object plane by an array of *pixels* located at positions  $\mathbf{r}_o(k)$ , with the integer  $k$  labeling the pixels. Different signals are emitted from different pixel positions, which play the role of an array of independent channel inputs. It follows from Eq. (7) that the input from the  $k$ th pixel is mapped to an output field at the image plane with spatial amplitudes

$$U_i^{(k)}(\mathbf{r}_i) = T(\mathbf{r}_i, \mathbf{r}_o(k)) U_o^{(k)}. \quad (12)$$

Let us notice that, even though the action of the channel is identical for all the input pixels, the output fields are not mutually independent. In fact, a pair of output fields, corresponding to the  $k$ th and  $k'$ th inputs have a nonvanishing spatial overlap,

$$C_{k,k'} := \frac{\iint d^2\mathbf{r}_i U_i^{(k)}(\mathbf{r}_i) U_i^{(k')*}(\mathbf{r}_i)}{U_o^{(k)} U_o^{(k')*}}; \quad (13)$$

that is,

$$C_{k,k'} = \iint d^2\mathbf{r}_i T(\mathbf{r}_i, \mathbf{r}_o(k)) T^*(\mathbf{r}_i, \mathbf{r}_o(k')). \quad (14)$$

The overlap between output signals may cause interference, which in turn produces distortion and loss of information in the communication via the optical channel. In particular, the overlap with the output field generated by the  $k$ th input signal induces noise in the detection of the  $k'$ th output. If the overlap between the two output fields is not negligible—that is, diffraction produces sensible effects—the noise affecting the  $k'$ th output field turns out to be highly correlated with the input signal at the  $k$ th pixel.

Introducing the dimensionless variable  $\tilde{\mathbf{r}} := \mathbf{r}/R$  (here  $R$  is the linear extension of the entrance pupil) and using the expression in Eq. (8) for the transfer function, we get the following expression for the output signal overlap,

$$C_{k,k'} = \frac{e^{i\delta\vartheta}}{x_R^2} \iint d^2\tilde{\mathbf{r}} P(\tilde{\mathbf{r}}) e^{-i2\pi \frac{[\mathbf{r}_o(k) - \mathbf{r}_o(k')]}{x_R} \cdot \tilde{\mathbf{r}}}, \quad (15)$$

from which it is evident that the spatial overlap between the two output fields is determined by the Rayleigh length of the apparatus:

$$x_R = \frac{\lambda D_o}{R}. \quad (16)$$

For instance, in the case of a circular pupil of radius  $R$ , we obtain

$$C_{k,k'} = \frac{e^{i\delta\vartheta}}{x_R} \frac{J_1(2\pi |\mathbf{r}_o(k) - \mathbf{r}_o(k')|/x_R)}{|\mathbf{r}_o(k) - \mathbf{r}_o(k')|}. \quad (17)$$

In conclusion, the Rayleigh length, which quantifies the amount of diffraction in the optical system, also quantifies the degree of correlations in the optical communication channel. The corresponding quantum memory channel manifests *intersymbol interference* effects and is qualitatively analogous to those studied in Refs. [29,33].

#### IV. THE QUANTUM CHANNEL

The light field at the object and image planes can be quantized according to standard canonical quantization. In order to derive the quantum version of the input/output relations in Eq. (7) we first identify a proper set of normal modes at the input and output field and proceed along the lines detailed in Sec. II.

We assume that information is encoded in the object plane on a square of length  $L$ , creating an image on the image plane which (in the geometric optics approximation) is contained in a square of size  $ML$ . We hence introduce the field variables

$$U_o(\mathbf{n}_o) := \frac{1}{L} \iint d^2 \mathbf{r}_o e^{-i2\pi(\frac{\mathbf{n}_o \cdot \mathbf{r}_o}{L} - \frac{|\mathbf{r}_o|^2}{2\lambda D_o} - \frac{D_o}{\lambda})} U_o(\mathbf{r}_o),$$

$$U_i(\mathbf{n}_i) := \frac{1}{ML} \iint d^2 \mathbf{r}_i e^{-i2\pi(\frac{\mathbf{n}_i \cdot \mathbf{r}_i}{ML} + \frac{|\mathbf{r}_i|^2}{2\lambda D_i} + \frac{D_i}{\lambda})} U_i(\mathbf{r}_i),$$
(18)

where the integral over  $\mathbf{r}_o$  is restricted to the surface of area  $L \times L$  which encircles the object, while the integral over  $\mathbf{r}_i$  is restricted to the surface of area  $ML \times ML$  which defines the receiving screen, and where  $\mathbf{n}_o$  and  $\mathbf{n}_i$  are vectors having two integer components. The functions  $U_o(\mathbf{n}_o)$  and  $U_i(\mathbf{n}_i)$  express the field components of transverse momentum  $2\pi \mathbf{n}_o/L$  and  $2\pi \mathbf{n}_i/(ML)$ , respectively at the object and image plane. Substituting Eqs. (18) into (7), and using (8), we write the input/output relations in the form

$$U_i(\mathbf{n}_i) = \sum_{\mathbf{n}_o} T_{\mathbf{n}_i, \mathbf{n}_o} U_o(\mathbf{n}_o),$$
(19)

where the transfer matrix  $T_{\mathbf{n}_i, \mathbf{n}_o}$  reads

$$T_{\mathbf{n}_i, \mathbf{n}_o} = \frac{1}{\lambda^2 D_o D_i} \iint d^2 \mathbf{r} P(\mathbf{r}) \Delta_{\mathbf{n}_i, \mathbf{n}_o}(\mathbf{r}),$$
(20)

with

$$\Delta_{\mathbf{n}_i, \mathbf{n}_o}(\mathbf{r}) = \frac{1}{ML^2} \iint d^2 \mathbf{r}_o e^{i2\pi(\frac{\mathbf{n}_o}{L} + \frac{M\mathbf{r}}{\lambda D_i}) \cdot \mathbf{r}_o} \times \iint d^2 \mathbf{r}_i e^{-i2\pi(\frac{\mathbf{n}_i}{ML} + \frac{\mathbf{r}}{\lambda D_i}) \cdot \mathbf{r}_i}.$$
(21)

Finally, we consider the *singular value decomposition* of the transfer matrix,

$$T_{\mathbf{n}_i, \mathbf{n}_o} = \sum_{\mathbf{n}} \mathcal{V}_{\mathbf{n}_i, \mathbf{n}} \sqrt{\eta_{\mathbf{n}}} \mathcal{U}_{\mathbf{n}, \mathbf{n}_o},$$
(22)

where, as in Eq. (2),  $\mathcal{U}_{\mathbf{n}, \mathbf{n}_o}$ ,  $\mathcal{V}_{\mathbf{n}_i, \mathbf{n}}$  are unitary matrices and  $\{\sqrt{\eta_{\mathbf{n}}}\}$  are the *singular values* of the matrix  $T_{\mathbf{n}_i, \mathbf{n}_o}$ , taking values in the interval  $[0, 1]$ . A set of input and output field variables are hence defined as follows:

$$\tilde{U}_o(\mathbf{n}) := \sum_{\mathbf{n}_o} \mathcal{U}_{\mathbf{n}, \mathbf{n}_o} U(\mathbf{n}_o),$$
(23)

$$\tilde{U}_i(\mathbf{n}) := \sum_{\mathbf{n}_i} \mathcal{V}_{\mathbf{n}_i, \mathbf{n}}^* U_i(\mathbf{n}_i).$$
(24)

It follows from Eq. (22) that they satisfy the identities

$$\tilde{U}_i(\mathbf{n}) = \sqrt{\eta_{\mathbf{n}}} \tilde{U}_o(\mathbf{n}).$$
(25)

In other words, the field variables  $\tilde{U}_o(\mathbf{n})$  are independently, but non-necessarily identically, transmitted to the output variables

$\tilde{U}_i(\mathbf{n})$ . The effect of the channel is to attenuate the  $\mathbf{n}$ th variable by a factor  $\eta_{\mathbf{n}}$ .

We can now promote the output and input field variables to the rank of quantum operators by substituting

$$\tilde{U}_o(\mathbf{n}) \rightarrow \sqrt{\hbar\omega/2} a_{\mathbf{n}}, \quad \tilde{U}_o^*(\mathbf{n}) \rightarrow \sqrt{\hbar\omega/2} a_{\mathbf{n}}^\dagger,$$
(26)

$$\tilde{U}_i(\mathbf{n}) \rightarrow \sqrt{\hbar\omega/2} b_{\mathbf{n}}, \quad \tilde{U}_i^*(\mathbf{n}) \rightarrow \sqrt{\hbar\omega/2} b_{\mathbf{n}}^\dagger,$$
(27)

where  $\omega = 2\pi c/\lambda$  is the frequency, and imposing the canonical commutation relations:

$$[a_{\mathbf{n}}, a_{\mathbf{n}'}^\dagger] = \delta_{\mathbf{n}, \mathbf{n}'},$$
(28)

$$[b_{\mathbf{n}}, b_{\mathbf{n}'}^\dagger] = \delta_{\mathbf{n}, \mathbf{n}'}.$$
(29)

The preservation of canonical commutation relations requires to invoke a set of canonical noise variables  $\{\xi_{\mathbf{n}}, \xi_{\mathbf{n}}^\dagger\}$  and to write the quantum version of Eq. (25) as

$$b_{\mathbf{n}} = \sqrt{\eta_{\mathbf{n}}} a_{\mathbf{n}} + \sqrt{1 - \eta_{\mathbf{n}}} \xi_{\mathbf{n}}.$$
(30)

This set of input/output relations, together with their Hermitian conjugates, characterizes, upon evaluation of the transmissivities  $\eta_{\mathbf{n}}$ , the quantum description of the optical channel.

#### V. CAPACITY OF THE OPTICAL QUANTUM COMMUNICATION CHANNEL

The input/output relations for the quantum description of the channel which have been derived in Eq. (30) formally qualify the optical system as a *broadband lossy channel*: a multimode channel in which a collection of bosonic modes is transmitted with corresponding efficiencies. This model has been characterized from the information-theoretical viewpoint in Refs. [22,23], where the capacities of the channel for transmitting classical and quantum information have been established.

The number of modes which are transmitted through the channel is virtually infinite. Actually, due to the finiteness of the entrance pupil, only a finite number of modes has nonzero transmissivity. The values of the transmissivities  $\eta_{\mathbf{n}}$  can be numerically estimated by first computing the elements of the transfer matrix  $T_{\mathbf{n}_i, \mathbf{n}_o}$ , and then its singular values. Indeed, the matrix in Eq. (21) can be rewritten in terms of the ratio  $L/x_R$ , and an analytical solution for the values of the effective transmissivities can be deduced in the following limits, namely,

$$L \ll x_R, \quad \text{FAR FIELD},$$
(31)

$$L \gg x_R, \quad \text{NEAR FIELD}.$$
(32)

First of all, we notice that in the far-field case Eq. (21) reads

$$\Delta_{\mathbf{n}_i, \mathbf{n}_o} \simeq ML^2 \delta_{\mathbf{n}_i, \mathbf{0}} \delta_{\mathbf{n}_o, \mathbf{0}},$$
(33)

where  $\delta$  denotes the Kronecker symbol. This expression in turn leads to

$$T_{\mathbf{n}_i, \mathbf{n}_o} \simeq \pi \left( \frac{L}{x_R} \right)^2 \delta_{\mathbf{n}_i, \mathbf{0}} \delta_{\mathbf{n}_o, \mathbf{0}};$$
(34)

that is, in the far-field regime only one mode is transmitted through the optical channel, and it is attenuated by a factor  $\simeq \pi^2 (L/x_R)^4$ . At least for optical frequencies it is reasonable



to assume that the noise modes in Eq. (30) are not populated. Under this assumption, using the result of Ref. [22], we are led to the following expression for the classical capacity of the optical channel:

$$C_{\text{ff}} = g\left(\frac{\pi^2 L^4}{x_R^4} \bar{n}\right), \quad (35)$$

where  $\bar{n}$  denotes the mean number photons at the object plane. The above calculations refer to the case of scalar field. Polarization can be included by doubling the total number of modes. In this case Eq. (35) will then be replaced by

$$C_{\text{ff}}^{\text{pol.}} = 2g\left(\frac{\pi^2 L^4}{2x_R^4} \bar{n}\right), \quad (36)$$

where the factor 2 which multiplies the  $g$  function comes from the fact that now there are two modes which can efficiently propagate, while the extra factor 1/2 in the argument of  $g$  comes from the fact that the available energy must be equipartitioned between them. Analogously, the quantum capacity can be computed according to Ref. [23].

Let us now consider the near-field limit,  $L \gg x_R$ . In this regime we can approximate

$$\Delta_{\mathbf{n}_i, \mathbf{n}_o}(\mathbf{r}) \simeq \lambda^2 D_o D_i \delta_{\mathbf{n}_i, \mathbf{n}_o} \delta^{(2)}\left(\mathbf{r} + \frac{\lambda D_o \mathbf{n}_o}{L}\right), \quad (37)$$

where  $\delta^{(2)}$  indicates the two-dimensional Dirac function. It follows that

$$T_{\mathbf{n}_i, \mathbf{n}_o} \simeq \delta_{\mathbf{n}_i, \mathbf{n}_o} P\left(\frac{\lambda D_o}{L} \mathbf{n}_o\right). \quad (38)$$

Within this approximation the transfer matrix is diagonal; hence, the singular values coincide with its diagonal entries. For a circular pupil of radius  $R$ , we obtain the following values for the transmissivities:

$$\eta_{\mathbf{n}} \simeq \begin{cases} 1 & \text{for } |\mathbf{n}| < L/x_R, \\ 0 & \text{for } |\mathbf{n}| > L/x_R. \end{cases} \quad (39)$$

We deduce that, in the near-field regime, the number of transmitted modes per surface unit is approximatively equal to  $\pi/x_R^2$ , each being transmitted with approximatively unit efficiency. Equivalently we can say that the total number of modes which are transferred with unit efficiency is equal to

$$\nu \simeq \pi(L/x_R)^2. \quad (40)$$

We are now in the condition of computing the capacity. Denoting by  $\bar{n}$  the average number of photons impinging on the surface, the capacity has the form Ref. [34]

$$C_{\text{nf}} = \nu g(\bar{n}/\nu) = \frac{\pi L^2}{x_R^2} g\left(\frac{x_R^2}{\pi L^2} \bar{n}\right), \quad (41)$$

where we used the fact that the maximum transfer is obtained when  $\bar{n}$  is equipartitioned among all transmitted modes. It is worth stressing that, since the modes employed in the transmission are perfectly transmitted, the classical capacity (expressed in *bits*) coincides with the quantum capacity (expressed in *qubits*). As before, our result can be generalized to include also the polarization degree of freedom obtaining

$$C_{\text{nf}}^{\text{pol.}} = \frac{2\pi L^2}{x_R^2} g\left(\frac{x_R^2}{2\pi L^2} \bar{n}\right). \quad (42)$$

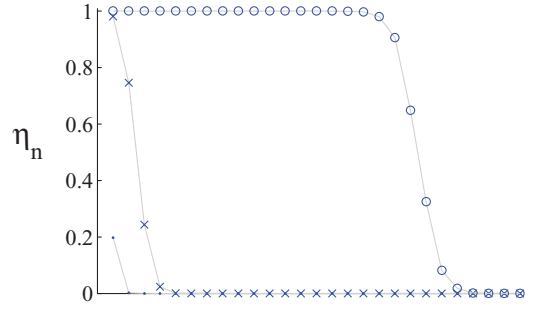


FIG. 2. (Color online) The effective transmissivities  $\eta_{\mathbf{n}}$ , for different value of the ratio  $L/x_R$ . Dots,  $L/x_R = 0.1$  (far field); crosses,  $L/x_R = 1$ ; circles,  $L/x_R = 10$  (near field). The figure refers to a one-dimensional setting, in which information is encoded at the object plane along an infinite strip of size  $L$ , and diffraction is caused by an infinitely long slit of size  $2R$ .

To evaluate the capacity for a generic value of the ratio  $L/x_R$ , it is necessary to numerically diagonalize the transfer matrix  $T$ . For the sake of simplicity, here we present an example of lower dimensionality, in which information is encoded at the object plane along an infinite strip of size  $L$ , and diffraction is caused by an infinitely long slit of size  $2R$ . The analysis of such 1D system is analogous to the 2D one, yielding the following expressions for the far-field and near-field capacities. In the far-field limit we have

$$C_{\text{ff}}^{(1D)} = g\left(\frac{2L}{x_R} \bar{n}\right), \quad (43)$$

and in the near-field limit

$$C_{\text{nf}}^{(1D)} = \frac{2L}{x_R} g\left(\frac{x_R}{2L} \bar{n}\right). \quad (44)$$

Figure 2 shows the transmissivities for several values of the ratio  $L/x_R$  for the one-dimensional problem. Figure 3 shows the capacity as function of the ratio  $L/x_R$ , compared with the limiting expressions of Eqs. (43) and (44).

## VI. ENHANCED QUANTUM COMMUNICATION VIA OPTICAL REFOCUSING

For a fair comparison between the optical communication through the optical system and the free-space one, we consider the case of free-space communication under the hypotheses that light is emitted by an object of surface  $L^2$ , propagates by a distance  $D = D_o + D_i = D_o(1 + M)$ , and is finally detected on a surface of size  $(ML)^2$ . This setting is depicted in Fig. 1(b). The light propagation, in both the classical and the quantum regimes, is characterized by the Fresnel number associated to this setting, that is,  $\mathcal{F} = M^2 L^4 / (\lambda D)^2$  (see [13] and references therein). In the far-field limit,  $\mathcal{F} \ll 1$ , only one mode is transmitted, with a corresponding transmissivity equal to the Fresnel number. On the other hand, in the near-field limit,  $\mathcal{F} \gg 1$ ,  $\mathcal{F}$  equals the number of modes which are transmitted with unit transmissivity. For these two regimes we can hence compute the free-space classical capacity according to Ref. [22]. By comparison with Eqs. (35) and (41), it follows that the presence of the radius- $R$  lens enhances the

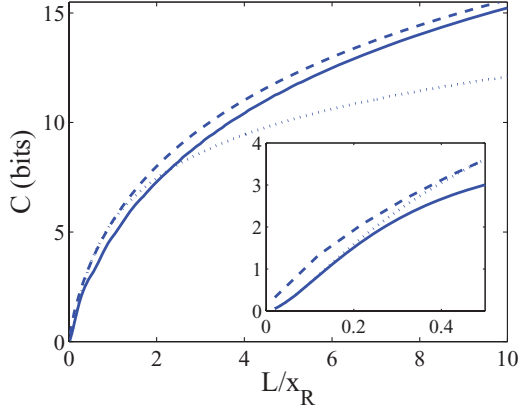


FIG. 3. (Color online) The plot shows the capacity (in the monochromatic case) as function of the ratio  $L/x_R$ , for  $\bar{n} = 4$ . The figure refers to a one-dimensional setting, in which information is encoded at the object plane along a straight line of length  $L$ , and diffraction is caused by an infinitely long slit of size  $2R$ . The solid line is the exact value of the capacity computed by numerical evaluation of the set of effective transmissivities. The dashed line indicates the approximation for near-field limit ( $L/x_R \gg 1$ ). The dotted line is the approximation for the far-field limit ( $L/x_R \ll 1$ ). The inset is a magnification of the far-field regime.

classical capacity over the free-space propagation only for not-too-large  $M$ , that is, for not-too-large imaging plane [specifically when  $\pi R/x_R > M/(1+M)$  in the far field and when  $\pi^{1/2}R/L > M/(1+M)$  in the near-field limit]. This rather counterintuitive effect originates from the simplifying assumption we made in writing Eq. (8) which implicitly states that the only light rays reaching the image plane are those which pass through the pupil, while the other are lost. Clearly the presence of such loss mechanism (which is not accounted for in the free-space calculation) is unimportant as long as the image plane is small, while it becomes relevant for a large imaging screen: This is exactly where the free-space starts to outperform the propagation through the lens.

Below we present a comparison between the performances of the refocusing apparatus, scenario (a), and those of the free-space propagation case, scenario (b). The goal is to produce results which are not affected by the approximation we made in writing Eq. (8) (i.e., the fact that we have implicitly assumed that all photons which do not hit the lens will not be transferred on the imaging plane). In order to do that, we also consider a third scenario, denoted by (c), which is depicted in Fig. 1(c).

#### A. Far-field regime for scenario (a)

Let us first consider the case in which the scenario (a) is operated in the far-field regime (31), which, according to Eq. (16), corresponds to have

$$\lambda \gg \frac{LR}{D_o}. \quad (45)$$

As already seen in the previous section, under this condition scenario (a) is characterized by having a single mode transmitted from the object plane to the image plane with an effective

transmissivity,

$$\eta_{(a)} = \pi^2 (L/x_R)^4 = \pi^2 \left( \frac{LR}{\lambda D_o} \right)^4 \ll 1. \quad (46)$$

In scenario (b), the field propagates freely from the object plane to the image plane. In this case the far-field regime is equivalent to impose

$$\lambda \gg \frac{LML}{D} = \frac{L^2}{D_o} \frac{M}{M+1}, \quad (47)$$

which, in principle, is independent from the far-field condition (45) for (a). Under condition (47) also (b) will admit the propagation of a single mode which is now attenuated by

$$\eta_{(b)} = \pi \left( \frac{L_o L_i}{\lambda D} \right)^2 = \pi \left( \frac{M}{M+1} \right)^2 \left( \frac{L^2}{\lambda D_o} \right)^2 \ll 1, \quad (48)$$

where  $L_o = L$  is the dimension of the object plane,  $L_i = ML$  the dimension of the image plane, and  $D = D_o + D_i$  is the distance between them. Then, assuming that both (45) and (47) hold, the ratio between the transmissivities is

$$r_1 = \frac{\eta_{(a)}}{\eta_{(b)}} = \pi \left( \frac{R^2}{\lambda D_o} \right)^2 \left( \frac{M+1}{M} \right)^2, \quad (49)$$

As already noticed this is not always larger than one: Indeed there is a condition which  $M, R, D_o, \lambda$  have to satisfy for this to happen. We now show that such condition is equivalent to impose that the loss induced by the pupil should be negligible. To do so, consider the alternative scenario (c), in which the field propagates from the object plane to the image plane while instead of the lens we have just a hole in the absorbing screen of the pupil. This configuration can be treated by analyzing separately the free-space propagation from the object plane to the absorbing screen ( $o \rightarrow s$ ) and the free-space propagation from the absorbing screen to the imaging plane ( $s \rightarrow i$ ). We notice that the condition Eq. (45) imposes that both these propagations take place in the far-field regime [35]. Therefore, we can conclude that, under the condition (45), in scenario (c) there will be a single propagating mode ( $o \rightarrow s \rightarrow i$ ). It is attenuated by a factor

$$\eta_{(c)}^{(o \rightarrow s)} = \pi \left( \frac{LR}{\lambda D_o} \right)^2 \quad (50)$$

in the section ( $o \rightarrow s$ ) and by

$$\eta_{(c)}^{(s \rightarrow i)} = \pi \left( \frac{RML}{\lambda D_i} \right)^2 = \pi \left( \frac{LR}{\lambda D_o} \right)^2 \quad (51)$$

in the section ( $s \rightarrow i$ ). The overall attenuation cannot be bigger than the product of the two factors; that is,

$$\eta_{(c)} \leq \eta_{(c)}^{(o \rightarrow s)} \eta_{(c)}^{(s \rightarrow i)} = \pi^2 \left( \frac{LR}{\lambda D_o} \right)^4 = \eta_{(a)}. \quad (52)$$

Now, if the presence of the absorbing screen around the pupil has to be negligible, then we must have that the loss that it induces is equal to the one of free-space propagation. Since  $\eta_{(c)} \leq \eta_{(a)}$ , this implies that the regime in which we can neglect the effect of absorbing screen is exactly the one in which  $r_1$  is greater than 1. In other words, the detrimental effects we see

for  $r_1 < 1$  simply correspond to the screen's absorption. As a final remark we also observe that the condition  $r_1 > 1$  plus the far-field regime (45) for (a) enforce the far-field regime (47) for the free-space propagation; indeed,

$$\begin{aligned} \frac{\lambda D_o}{L^2} \frac{M+1}{M} &= \left( \frac{\lambda^2 D_o^2}{R^2 L^2} \right) \left( \frac{R^2}{\lambda D_o} \right) \frac{M+1}{M} \\ &= \left( \frac{\lambda^2 D_o^2}{R^2 L^2} \right) \sqrt{\frac{r_1}{\pi}} > \left( \frac{\lambda^2 D_o^2}{R^2 L^2} \right) \gg 1. \end{aligned} \quad (53)$$

We now compare the performances of scenarios (a) and (b) in terms of capacities by computing the ratio,

$$G_1 = \frac{C_{(a)}}{C_{(b)}} = \frac{g(\eta_{(a)} \bar{n})}{g(\eta_{(b)} \bar{n})} = \frac{g(r_1 \eta_{(b)} \bar{n})}{g(\eta_{(b)} \bar{n})}. \quad (54)$$

This is a monotonic function of  $\bar{n}$ , with  $G_1 \simeq r_1$  for  $\bar{n} \ll 1$  (faint signal limit) and  $G_1 \simeq 1$  for  $\bar{n} \gg 1$  (semiclassical limit). The enhancement in the transmission rate provided by the optical refocusing system persists in the presence of background thermal noise. In such a case, by encoding classical information into coherent states, the expression  $g(\eta \bar{n})$  has to be replaced by  $g(\eta \bar{n} + \bar{n}_{\text{th}}) - g(\bar{n}_{\text{th}})$ , where  $\bar{n}_{\text{th}}$  denotes the mean number of thermal background photons per transmitted mode [16], yielding  $G_1 \simeq r_1$  even in the very noisy limit  $\bar{n}_{\text{th}} \gg \bar{n}$ .

### B. Near-field regime for scenario (a)

The near-field regime for scenario (a) is defined by the inequality (32) which rewrites also as

$$\lambda \ll \frac{LR}{D_o}. \quad (55)$$

From the discussion of Sec. V we know that in this regime the scenario (a) is characterized by having a collection of  $\nu_{(a)}$  modes which are perfectly transmitted from the object plane to the image plane,

$$\nu_{(a)} = \pi (L/x_R)^2 = \pi \left( \frac{LR}{\lambda D_o} \right)^2 \gg 1. \quad (56)$$

In a similar way the near-field regime for the scenario (b) takes place when

$$\lambda \ll \frac{L_o L_i}{D} = \frac{L^2}{D_o} \frac{M}{M+1}, \quad (57)$$

which is independent from the near-field condition for (a) (55). Under this condition also (b) admits  $\nu_{(b)}$  modes which are perfectly transferred, with

$$\nu_{(b)} = \pi \left( \frac{L_o L_i}{\lambda D} \right)^2 = \pi \left( \frac{M}{M+1} \right)^2 \left( \frac{L^2}{\lambda D_o} \right)^2 \gg 1. \quad (58)$$

Assume then that both (55) and (57) hold and define the quality factor

$$r_2 := \frac{\nu_{(a)}}{\nu_{(b)}} = \left( \frac{M+1}{M} \right)^2 \left( \frac{R}{L} \right)^2. \quad (59)$$

As in the case of Sec. VIA, if there are no losses introduced by the absorption of the rays propagating outside the lens, we must have  $r_2 \geq 1$ . To see this let us consider what happens in scenario (c). We first notice that the condition (55) guarantees

that both the propagations ( $o \rightarrow s$ ) and ( $s \rightarrow i$ ) are in the near-field regime. The number of modes that they allow for perfect propagation is given by

$$\nu_{(c)}^{(o \rightarrow s)} = \nu_{(c)}^{(s \rightarrow i)} = \pi \left( \frac{LR}{\lambda D_o} \right)^2 = \nu_{(a)}. \quad (60)$$

Notice that they are identical, due to the fact that  $L_i/D_i = L/D_o$ . This implies that  $\nu_{(c)} \leq \nu_{(a)}$ . Then, it is clear that the presence of the pupil is negligible only when  $\nu_{(c)}$  is larger than  $\nu_{(b)}$ , that is,  $r_2 \geq 1$ , therefore proving the thesis.

We remark that the condition  $r_2 \geq 1$ , together with the near-field condition for the scenario (a) [Eq. (55)] is not sufficient to guarantee the near-field condition for scenario (b). Indeed, we notice that

$$\frac{L^2}{\lambda D_o} \frac{M}{M+1} = \frac{LR}{\lambda D_o} \left( \frac{M}{M+1} \frac{L}{R} \right), \quad (61)$$

which by itself does not imply the near-field condition for (b), that is, Eq. (57). That yields the possibility to have (a) in near field and (b) in either near field or far field.

Let us examine the two cases.

(i) First assume that both (a) and (b) are in the near-field regime (of course, under the constraint that  $r_2 > 1$  to exclude the absorption by the pupil). The ratio between the capacities becomes

$$\begin{aligned} G_2 &= \frac{C_{(a)}}{C_{(b)}} = \frac{\nu_{(a)} g(\bar{n}/\nu_{(a)})}{\nu_{(b)} g(\bar{n}/\nu_{(b)})} \\ &= r_2 \frac{g(\bar{n}/\nu_{(a)})}{g(r_2 \bar{n}/\nu_{(a)})}, \end{aligned} \quad (62)$$

which is a monotonic function of  $\bar{n}$ , with  $G_2 \simeq 1$  for  $\bar{n} \ll 1$  (faint signal limit) and  $G_2 \simeq r_2$  for  $\bar{n} \gg 1$  (semiclassical limit).

(ii) Then assume that (a) is near field and (b) is far field, that is,

$$\frac{L^2}{D_o} \frac{M}{M+1} \ll \lambda \ll \frac{LR}{D_o}. \quad (63)$$

Under these conditions one can immediately verify that the presence of the absorbing screen does not affect the performances of scenario (b), and we can make a fair comparison. In this case the gain becomes

$$G_3 = \frac{C_{(a)}}{C_{(b)}} = \frac{\nu_{(a)} g(\bar{n}/\nu_{(a)})}{g(\eta_{(b)} \bar{n})}, \quad (64)$$

giving  $G_3 \simeq 1/\eta_{(b)} \gg 1$  for  $\bar{n} \ll 1$  (faint signal limit) and  $G_3 \simeq \nu_{(a)} \gg 1$  for  $\bar{n} \gg 1$  (semiclassical limit). In the presence



of noisy thermal environment [16], the expressions  $g(\eta\bar{n})$  and  $g(\bar{n}/\nu)$  have to be replaced by  $g(\eta\bar{n} + \bar{n}_{\text{th}}) - g(\bar{n}_{\text{th}})$  and  $g(\bar{n}/\nu + \bar{n}_{\text{th}}) - g(\bar{n}_{\text{th}})$ , respectively. The advantages of optical refocusing hence persist even in the very noisy limit  $\bar{n}_{\text{th}} \gg \bar{n}$ , yielding  $G_3 \simeq 1/\eta_{(b)}$ .

## VII. COMMUNICATION WITH NONMONOCHROMATIC LIGHT

Until now we have considered the case of monochromatic light, we now want to compute the communication capacity of the optical system by assuming nonmonochromatic light. An input signal over a time interval  $T$  can be expanded in terms of monochromatic components at frequencies  $\omega_j = 2\pi j/T$ , with  $j = 0, 1, \dots, \infty$ . If the optical system is characterized by a certain bandwidth extending from  $\Omega$  to  $\Omega + \delta\Omega$ , only a finite number of components are transmitted, corresponding to the frequencies  $\omega_n$  such that  $\Omega \leq \omega_j \leq \Omega + \delta\Omega$ . Each monochromatic component contributes with a term as in Eq. (41), with  $x_R = \lambda_j D_o/R = 2\pi c D_o/(\omega_j R)$ . In the following we work under the assumption that the frequency modes are either all in the far-field regime or all in the near-field one.

### A. Far field

If all the transmitted frequency modes fulfill the far-field condition (31), we must have

$$L \ll x_R = 2\pi c D_o/(\omega_j R), \quad (65)$$

for all  $\omega_j$ . Consequently, the results of Eq. (35) can be applied to the whole spectrum. This allows us to derive the following expression for the capacity

$$C_{\text{ff}} = \sum_{\Omega \leq \omega_j \leq \Omega + \delta\Omega} g(\alpha \omega_j^4 \bar{n}_j), \quad (66)$$

where

$$\alpha := \pi^2 \left( \frac{LR}{2\pi c D_o} \right)^4, \quad (67)$$

and the parameter  $\bar{n}_j$  counts the average number of photons at frequency  $\omega_j$ . If a mean power  $P$  is employed, the parameters  $\bar{n}_j$  ought to obey the constraint

$$\frac{1}{T} \sum_{\Omega \leq \omega_j \leq \Omega + \delta\Omega} \hbar \omega_j \bar{n}_j = P. \quad (68)$$

The maximization over photon number distributions satisfying the input energy constraint can be worked out by the Lagrange method, yielding the optimal photon number distribution

$$\bar{n}_j = [\alpha \omega_j^4 (2^{\frac{\mu \hbar}{\alpha \omega_j^3 T}} - 1)]^{-1}, \quad (69)$$

with  $\mu$  being the Lagrange multiplier. For sufficiently large  $T$  we can approximate the summations with integrals, and the channel capacity reads

$$C_{\text{ff}} = \frac{T}{2\pi} \int_{\Omega}^{\Omega + \delta\Omega} d\omega g\left(\frac{1}{2^{\frac{\mu \hbar}{\alpha \omega^3 T}} - 1}\right), \quad (70)$$

where the value of the Lagrange multiplier is determined by the implicit equation

$$P = \frac{\hbar}{2\alpha\pi} \int_{\Omega}^{\Omega + \delta\Omega} \frac{d\omega}{\omega^3} (2^{\frac{\mu \hbar}{\alpha \omega^3 T}} - 1)^{-1}. \quad (71)$$

A closed form for the classical capacity can be found in the narrowband limit,  $\delta\Omega \ll \Omega$ , in which we obtain the approximate expression

$$C_{\text{ff}}^{\text{nb}} \simeq \frac{T\delta\Omega}{2\pi} g\left(\frac{2\pi P\alpha\Omega^3}{\hbar\delta\Omega}\right). \quad (72)$$

### B. Near field

Let us now assume that all the frequency modes fulfill the near-field condition (32), that is,

$$L \gg x_R = 2\pi c D_o/(\omega_j R). \quad (73)$$

We can hence apply Eq. (41) to the whole spectrum, which allows us to write the channel classical capacity as follows:

$$C_{\text{nf}} = \sum_{\Omega \leq \omega_j \leq \Omega + \delta\Omega} \nu_j g\left(\frac{\bar{n}_j}{\nu_j}\right) \quad (74)$$

$$= \sum_{\Omega \leq \omega_j \leq \Omega + \delta\Omega} \beta \omega_j^2 g\left(\frac{\bar{n}_j}{\beta \omega_j^2}\right), \quad (75)$$

where  $\nu_j$  counts the number of transmitted modes of the frequency  $\omega_j$  [Eq. (40)],  $\bar{n}_j$  counts the average number of photon of that frequency, and where we have introduced

$$\beta := \pi \left( \frac{LR}{2\pi c D_o} \right)^2. \quad (76)$$

The optimization over the photon-number distribution under the constraint of total power  $P$  yields the optimal photon-number distribution

$$\bar{n}_j = \frac{\beta \omega_j^2}{2\mu \hbar \omega_j / T - 1}, \quad (77)$$

with  $\mu$  being the Lagrange multiplier. For sufficiently large  $T$  we can approximate the summations with integrals, and the channel capacity reads

$$\begin{aligned} C_{\text{nf}} &= \frac{\beta T}{2\pi} \int_{\Omega}^{\Omega + \delta\Omega} d\omega \omega^2 g\left(\frac{1}{2^{\mu \hbar \omega / T} - 1}\right) \\ &= \frac{\beta T}{2\pi q^3} \int_{q\Omega}^{q(\Omega + \delta\Omega)} dx x^2 g\left(\frac{1}{e^x - 1}\right), \end{aligned} \quad (78)$$

where we rescaled the Lagrange multiplier introducing the quantity  $q = \ln(2)\mu\hbar/T$ , which is determined by the implicit equation

$$P = \frac{\beta \hbar}{2\pi q^4} \int_{q\Omega}^{q(\Omega + \delta\Omega)} dx \frac{x^3}{e^x - 1}. \quad (79)$$

We can single out two limiting situations, the narrowband and the broadband limits, for which analytical expressions can be obtained.

### 1. Narrowband limit

In the narrowband limit,  $\delta\Omega \ll \Omega$ , we obtain

$$C_{\text{nf}}^{\text{nb}} \simeq \frac{\beta}{2\pi} T \Omega^2 \delta\Omega g\left(\frac{2\pi P}{\beta\hbar\Omega^3\delta\Omega}\right). \quad (80)$$

This can be cast in a more familiar form by noticing that in this limit the power  $P$  can be expressed as

$$P \simeq \frac{1}{T} \left(\frac{\delta\Omega T}{2\pi}\right) \hbar\Omega \bar{n}(\Omega), \quad (81)$$

where  $\delta\Omega T/(2\pi)$  is the total number of frequencies and  $\bar{n}(\Omega)$  is the density of mean photon number at frequency  $\Omega$ . Replacing this into Eq. (80) and using  $\beta\Omega^2 = \pi(L/x_R)^2$ , where  $x_R$  is the Rayleigh length of the frequency  $\Omega$ , we get

$$C_{\text{nf}}^{\text{nb}} \simeq \left(\frac{\delta\Omega T}{2\pi}\right) \pi \frac{L^2}{x_R^2} g\left(\frac{x_R^2}{\pi L^2} \bar{n}(\Omega)\right). \quad (82)$$

This expression shows that  $C_{\text{nf}}^{\text{nb}}$  coincides with the single frequency capacity (41), multiplied by the total number of frequencies  $\delta\Omega T/(2\pi)$ .

### 2. Broadband limit

In the broadband limit, we set  $\Omega + \delta\Omega \rightarrow +\infty$ , and we have

$$P \simeq \frac{\beta\hbar}{2\pi q^4} \mathcal{F}(q\Omega), \quad (83)$$

$$C_{\text{nf}}^{\text{bb}} \simeq \frac{\beta T}{2\pi q^3} \mathcal{G}(q\Omega), \quad (84)$$

with  $\mathcal{F}(z)$  and  $\mathcal{G}(z)$  being the following decreasing functions:

$$\mathcal{F}(z) := \int_z^\infty dx \frac{x^3}{e^x - 1}, \quad (85)$$

$$\mathcal{G}(z) := \int_z^\infty dx x^2 g\left(\frac{1}{e^x - 1}\right). \quad (86)$$

An analytical solution can be obtained by approximating  $q\Omega$  to zero. Notice that this is not formally correct if we want to preserve the condition (73) for all frequencies of the spectrum: However, since  $\mathcal{F}(z)$  and  $\mathcal{G}(z)$  are smooth in the proximity of  $z = 0$  the error becomes negligibly small. By close inspection of the Eqs. (85) and (86), however, it follows that the approximations  $\mathcal{F}(z) \simeq \mathcal{F}(0)$ ,  $\mathcal{G}(z) \simeq \mathcal{G}(0)$  are justified if  $z \lesssim 1$ , that is, for  $q\Omega \lesssim 1$ , which in turn implies

$$\frac{2\pi}{\beta\hbar} \frac{P}{\Omega^4} \gtrsim \mathcal{F}(0). \quad (87)$$

Under this assumptions it follows that the condition (73) is satisfied in the semiclassical regime  $P/(\hbar\Omega^2) \gg 1$ . Consequently, we can write

$$P \simeq \frac{\beta\pi^3\hbar}{30q^4}, \quad (88)$$

$$C_{\text{nf}}^{\text{bb}} \simeq \frac{\beta\pi^3 T}{45q^3} \log_2 e, \quad (89)$$

which yields

$$C_{\text{nf}}^{\text{bb}} \simeq \frac{\beta\pi^2 T}{3\sqrt[4]{15}} \left[\frac{2\pi P}{\beta\hbar}\right]^{3/4} \log_2 e. \quad (90)$$

These expressions are obtained by noticing that the integrals in Eqs. (85) and (86) can be written in terms of the Bernoulli numbers  $B_k$  by means of the identity (see, e.g., [36])

$$\int_0^\infty dx \frac{x^{2n-1}}{e^{px} - 1} = (-1)^{n-1} \left(\frac{2\pi}{p}\right)^{2n} \frac{B_{2n}}{4n}. \quad (91)$$

By comparing (90) with the capacity of a multimode Gaussian bosonic channel [11,22,37] we notice that the scaling in  $P$  is now changed (there it scales as  $P^{1/2}$ ). This is due to the fact that in our case each frequency has multiple degeneracies.

## VIII. CONCLUSION

We have computed the capacity of quantum optical communication through an optical system characterized by a finite entrance pupil. Our calculations provide general bounds on the efficiency of quantum optical communication taking into account the effects of light diffraction. This models a rather general situation in long-distance communication, where repeaters play the role of the optical system used to refocus the signal. More generally, any transfer of information which employ quantum degrees of freedom of light—from quantum key distribution [8–10] to quantum imaging [38], as well as quantum discrimination problems [39–42] and quantum reading [43–45]—requires the propagation through an optical system, and it is hence limited by diffraction.

We have argued that, when the optical system is used for information transmission, the effects of diffraction can be formally described as a quantum channel with correlated noise. It follows that correlated noise may affect all the quantum information protocols requiring propagation and detection of quantum light.

Finally, this formal equivalence has allowed us to apply tools that were developed in the framework of quantum memory channel characterization to the diffraction problem. In particular, this has allowed us to show that, under certain conditions, a converging optical apparatus can be used to achieve higher transmission rates than the free-space field propagation. The tradeoff between loss and diffraction determines the conditions under which the intuitive benefits of optical refocusing can be rigorously proven.

## ACKNOWLEDGMENTS

We acknowledge discussions with Lorenzo Maccone and Ciro Biancofiore. The research leading to these results has received funding from the European Commission's seventh Framework Programme (FP7/2007-2013) under Grant Agreement No. 213681 and by the Italian Ministry of University and Research under the FIRB-IDEAS Project No. RBID08B3FM. V.G. also acknowledges the support of Institut Mittag-Leffler (Stockholm), which he was visiting while part of this work was done. S.P. acknowledges the support of EPSRC (EP/J00796X/1) and the European Union (MOIF-CT-2006-039703).

- [1] T. C. Ralph and P. K. Lam, *Nat. Photon.* **3**, 671 (2009); R. Ursin *et al.*, *Nat. Phys.* **3**, 481 (2007).
- [2] S. L. Braunstein and P. van Loock, *Rev. Mod. Phys.* **77**, 513 (2005).
- [3] C. Weedbrook, S. Pirandola, R. Garcia-Patron, N. J. Cerf, T. C. Ralph, J. H. Shapiro, and Seth Lloyd, *Rev. Mod. Phys.* **84**, 621 (2012).
- [4] S. Lloyd and S. L. Braunstein, *Phys. Rev. Lett.* **82**, 1784 (1999).
- [5] S. L. Braunstein, *Phys. Rev. Lett.* **80**, 4084 (1998); S. Lloyd and Jean-Jacques E. Slotine, *ibid.* **80**, 4088 (1998).
- [6] D. Gottesman, A. Kitaev, and J. Preskill, *Phys. Rev. A* **64**, 012310 (2001).
- [7] A. Furusawa, J. L. Sørensen, S. L. Braunstein, C. A. Fuchs, H. J. Kimble, and E. S. Polzik, *Science* **282**, 706 (1998).
- [8] F. Grosshans, G. Van Assche, J. Wenger, R. Brouri, N. J. Cerf, and P. Grangier, *Nature (London)* **421**, 238 (2003).
- [9] C. Weedbrook, A. M. Lance, W. P. Bowen, T. Symul, T. C. Ralph, and P. K. Lam, *Phys. Rev. Lett.* **93**, 170504 (2004); A. M. Lance, T. Symul, V. Sharma, C. Weedbrook, T. C. Ralph, and P. K. Lam, *ibid.* **95**, 180503 (2005).
- [10] S. Pirandola, S. Mancini, S. Lloyd, and S. L. Braunstein, *Nat. Phys.* **4**, 726 (2008).
- [11] C. M. Caves and P. D. Drummond, *Rev. Mod. Phys.* **66**, 481 (1994).
- [12] H. P. Yuen and J. H. Shapiro, *IEEE Trans. Inf. Theory* **24**, 657 (1978).
- [13] J. H. Shapiro, *IEEE J. Sel. Top. Quantum Electron.* **15**, 1547 (2009).
- [14] B. Schumacher and M. D. Westmoreland, *Phys. Rev. A* **56**, 131 (1997); A. S. Holevo, *IEEE Trans. Inf. Theory* **44**, 269 (1998).
- [15] I. Devetak, *IEEE Trans. Inf. Theory* **51**, 44 (2005); S. Lloyd, *Phys. Rev. A* **55**, 1613 (1997).
- [16] A. S. Holevo and R. F. Werner, *Phys. Rev. A* **63**, 032312 (2001).
- [17] C. E. Shannon, *Bell Syst. Tech. J.* **27**, 379 (1948); **27**, 623 (1948).
- [18] A. S. Holevo, *Probl. Inf. Transm. (Engl. Transl.)* **43**, 1 (2007); F. Caruso, J. Eisert, V. Giovannetti, and A. S. Holevo, *New J. Phys.* **10**, 083030 (2008).
- [19] F. Caruso, V. Giovannetti, and A. S. Holevo, *New J. Phys.* **8**, 310 (2006).
- [20] S. Pirandola, S. L. Braunstein, and S. Lloyd, *Phys. Rev. Lett.* **101**, 200504 (2008).
- [21] S. Pirandola, R. Garcia-Patron, S. L. Braunstein, and S. Lloyd, *Phys. Rev. Lett.* **102**, 050503 (2009).
- [22] V. Giovannetti, S. Guha, S. Lloyd, L. Maccone, J. H. Shapiro, and H. P. Yuen, *Phys. Rev. Lett.* **92**, 027902 (2004).
- [23] M. M. Wolf, D. Pérez-García, and G. Giedke, *Phys. Rev. Lett.* **98**, 130501 (2007).
- [24] C. Lupo, S. Pirandola, P. Aniello, and S. Mancini, *Phys. Scr.*, **T 143**, 014016 (2011).
- [25] V. Giovannetti, S. Lloyd, L. Maccone, and J. H. Shapiro, *Phys. Rev. A* **69**, 052310 (2004).
- [26] V. Giovannetti, S. Guha, S. Lloyd, L. Maccone, J. H. Shapiro, B. J. Yen, and H. P. Yuen, *Quantum Inf. Comput.* **4**, 489 (2004).
- [27] V. W. S. Chan, *J. Lightw. Technol.* **21**, 2811 (2003); *IEEE J. Sel. Top. Quantum Electron.* **6**, 959 (2000); *J. Lightwave Technol.* **24**, 4750 (2006).
- [28] D. Kretschmann and R. F. Werner, *Phys. Rev. A* **72**, 062323 (2005).
- [29] C. Lupo, V. Giovannetti, and S. Mancini, *Phys. Rev. Lett.* **104**, 030501 (2010); *Phys. Rev. A* **82**, 032312 (2010).
- [30] H. Nyquist, *Trans. AIEE* **47**, 617 (1928); C. E. Shannon, *Proc. Inst. Radio Eng.* **37**, 10 (1949).
- [31] C. Lupo, V. Giovannetti, S. Pirandola, S. Mancini, and S. Lloyd, *Phys. Rev. A* **84**, 010303(R) (2011).
- [32] J. W. Goodman, *Introduction to Fourier Optics* (McGraw-Hill, New York, 1968).
- [33] G. Bowen, I. Devetak, and S. Mancini, *Phys. Rev. A* **71**, 034310 (2005).
- [34] The expression in Eq. (41) diverges in the limit of  $x_R \rightarrow 0$ . Clearly, that is an artifact due to the use of the paraxial approximation ( $R/D_o \ll 1$ ) in the derivation of the capacity's formula. Indeed, the free-space propagation of light acts as a filter which transmits only the transverse wave vector components satisfying  $2\pi \mathbf{n}_o/L < 2\pi/\lambda$  [32]. Thus, the capacity of the optical system cannot be larger than  $C = \frac{\pi L^2}{\lambda^2} g(\frac{\lambda^2 \bar{n}}{\pi L^2})$ .
- [35] Equation (45) defines the far-field regime for the free-space ( $o \rightarrow s$ ) propagation. Similarly, since the ratio between the ( $s \rightarrow i$ ) distance  $D_i$  and the dimension of the imaging plane  $ML$  are equal to  $D_o/L$  this condition defines also the far-field regime for the free-space ( $s \rightarrow i$ ) propagation.
- [36] I. S. Gradshteyn and I. M. Ryzhik, *Table of Integrals, Series, and Product* (Academic, New York, 2007).
- [37] H. P. Yuen and M. Ozawa, *Phys. Rev. Lett.* **70**, 363 (1993).
- [38] V. Giovannetti, S. Lloyd, L. Maccone, and J. H. Shapiro, *Phys. Rev. A* **79**, 013827 (2009).
- [39] S.-H. Tan, B. I. Erkmen, V. Giovannetti, S. Guha, S. Lloyd, L. Maccone, S. Pirandola, and J. H. Shapiro, *Phys. Rev. Lett.* **101**, 253601 (2008); S. Lloyd, *Science* **321**, 1463 (2008).
- [40] S. Pirandola and S. Lloyd, *Phys. Rev. A* **78**, 012331 (2008).
- [41] H. P. Yuen and R. Nair, *Phys. Rev. A* **80**, 023816 (2009).
- [42] S. Guha and B. I. Erkmen, *Phys. Rev. A* **80**, 052310 (2009); A. R. Usha Devi, and A. K. Rajagopal, *ibid.* **79**, 062320 (2009).
- [43] S. Pirandola, *Phys. Rev. Lett.* **106**, 090504 (2011).
- [44] R. Nair, *Phys. Rev. A* **84**, 032312 (2011); A. Bisio, M. Dall'Arno, and G. M. D'Ariano, *ibid.* **84**, 012310 (2011); R. Nair and B. J. Yen, *Phys. Rev. Lett.* **107**, 193602 (2011); O. Hirota, *arXiv:1108.4163*; M. Dall'Arno, A. Bisio, G. M. D'Ariano, M. Mikova, M. Jezek, and M. Dusek, *Phys. Rev. A* **85**, 012308 (2012).
- [45] S. Pirandola, C. Lupo, V. Giovannetti, S. Mancini, and S. L. Braunstein, *New J. Phys.* **13**, 113012 (2011).